CALIBRATION OF SCOUR MODELS USING ADVANCED SONAR TECHNOLOGY FOR BRIDGE SAFETY

James H. Miller, Gopu Potty,
Chuen Song-Chen and Christopher Baxter
University of Rhode Island

June 2005

URITC PROJECT NO. **000059**

PREPARED FOR

UNIVERSITY OF RHODE ISLAND
TRANSPORTATION CENTER

1. Report No	2. Government Accession No.	3. Recipient's Catalog No.
URITC FY03-05	N/A	N/A

4. Title and Subtitle	5. Report Date
Calibration of Scour Models using Advanced Sonar Technology for Bridge Safety	June 2005
	6. Performing Organization Code N/A

7. Authors(s)	8. Performing Organization Report No.
James Miller, Gopu Potty, Chuen-Song Chen and Christopher Baxter	N/A

9. Performing Organization Name and Address	10. Work Unit No. (TRAIS)
University of Rhode Island, Dept. of Ocean Engineering, Narragansett, RI 02882 (401) 874- 6540 miller@egr.uri.edu	N/A
	11. Contract or Grant No. URI 500230600000000059
	13. Type of Report and Period Covered Final

12. Sponsoring Agency Name and Address	14. Sponsoring Agency Code
University of Rhode Island Transportation Center Carlotti Administration Building, 75 Lower College Road Kingston, RI 02881	A study conducted in cooperation with U.S. DOT

15. Supplementary Notes
N/A

16. Abstract

Riverbed scour near bridge piers is a widespread problem which causes scour holes to develop, piers to fall and, ultimately, bridges to collapse. Measurement of riverbed scour and deposition near bridge piers are essential for the proper maintenance and safety of bridges. Scour processes have been extensively studied and mathematical models have been developed from physical models and field data. But scour depths predicted using these models could vary substantially when these models are applied outside the range of conditions for which they have been developed. Field measurements of scour depths are needed to put practical constraints and limits on these models. We conducted these field measurements using a number of underwater acoustic instruments and techniques. These instruments include depth sounder, side scan sonar, and sub-bottom profiler. These measurements were conducted aboard the Department of Ocean Engineering research vessel R/V CT-1 and another research vessel- R/V Quest. This will also then serve as a rapid assessment tool for scour and has the potential to compliment and/or replace inspection by divers.

17. Key Words	18. Distribution Statement
Scour at Bridges, Sonar, Acoustic Monitoring, Scour Prediction, Bridge Safety	No restrictions. This document is available to the Public through the URI Transportation Center, Carlotti Administration Building, 75 Lower College Rd., Kingston, RI 02881

19. Security Classif. (of this report)	20. Security Classif. (of this page)	21. No. of Pages	22. Price
Unclassified	Unclassified	**30**	N/A

Form DOT F 1700.7 (8-72) Reproduction of completed page authorized (art. 5/94)

TABLE OF CONTENTS

LIST OF FIGURES

1.0 INTRODUCTION

Measurement of riverbed scour and deposition near bridge piers are essential for the proper maintenance and safety of bridges. Scour processes have been extensively studied in the past and mathematical models have been developed from physical models and field data. Various field measurement techniques have also been studied for identifying and monitoring the scour process. Most of the instruments are based on acoustic principles since sound has been accepted as the best tool to explore underwater due to its excellent propagation characteristics in water (as opposed to light for example). Sonar technology has been making rapid strides over the years in pace with advances in underwater acoustics, signal processing and computational capability. Scour monitoring techniques based on sonar technology also have been updated over the years in parallel with this progress in sonar technology. The major objective of this project is to use latest sonar technology for identifying and monitoring the problem of scour around bridge piers. Surveys using sidescan sonars can provide an image of the vicinity of the bridge piers indicating the condition of the pier foundation (such as presence of scour, debris or displaced protective cover). As a rapid assessment tool, this can aid and sometimes replace physical inspection by divers. This will also provide some practical constraints and limits on the scour prediction models. As part of the project we conducted field measurements using a sidescan sonar at two locations – Newport and Sakkonnet River bridges in Rhode Island. Specific objectives that were addressed in this project include

- Investigate the various scour prediction models and their applicability to local conditions.
- Collect field measurements using a number of advanced acoustic instruments and techniques (forward looking sonar, downward looking sonars etc.). In addition other environmental measurements (current measurements) will also be taken.
- Calibrate the models using the field measurements taken.
- Investigate the effectiveness of acoustic measuring techniques as a rapid assessment tool.

It should be pointed out that more emphasis was placed on field measurements using the sidescan sonar in this study compared to other objectives. The data collected during this field study will have to be augmented by other data and model runs to fully achieve the third objective (calibrate the models using field measurements). The lessons learned in the present study will be very useful for future field programs and model studies especially in this region.

This report is organized as follows. Review of the scour problem and the instruments used to monitor scour is provided in the remainder of this section. A sidescan sonar manufactured by Edgetech was used for this study. Important features of the Edgtech side scan sonar used in the field study are also provided in Section 1. 4. Tidal currents dominate the two locations surveyed in this study. Section 2 provides details of scour analysis techniques for tidal waterways. The sidescan sonar was deployed in two locations as part of this study. Details of the field experiments conducted at Newport and Sakkonnet bridge sites are provided in Section 3. Section 4 concludes the report by discussing the results.

1.1 Scour Around Bridge Piers

Damage to bridge crossings during flood events endangers the lives of the traveling public and causes costly disruptions to traffic flow. The interruption to traffic flow can have devastating impacts on local economies that rely on bridge crossings for efficient transport of goods and services. Although submergence of bridge crossings is the leading cause of traffic disruption during flood events, the primary cause of bridge collapse is scouring of the streambed and banks and erosion of highway embankments. Scour is the erosion of waterway soils and sediment that provide support for bridge foundations.

Scour causes more bridge failures than all other processes combined. Adequate evaluation of the potential for bridge scour is essential for the assessment of the existing bridges. The lack of fundamental knowledge of stream and river system development and evolutionary processes, the widely varying conditions under which they develop, and the complexity of the scour mechanisms are major impediments to the formulation of highly accurate scour prediction models. Hence scour inspections are vital to the forecasting of future scour problems at existing bridges and must be incorporated as an integral part of the bridge evaluation process. Advances in scour prediction models must be correlated with inspection procedures by comparing the observations against predicted scour at the site.

An equilibrium pier scour depth (y_s) may be defined as the maximum scour depth attained after the bed around the pier has been exposed to given flow conditions for a sufficiently long time. The time to reach the equilibrium conditions may be very long (e.g., days). When the velocity of flow is low and/or the bed material is small the sediment transport upstream and down stream of the structure will be negligible. In this case sediment is entrained into the flow only in the immediate neighborhood of the structure. In this condition there is no refilling of the scour hole. Under more probable live bed conditions, sediment transported from the upstream of the structure may refill the scour hole, and a cyclic pattern of scour and refill may become established.

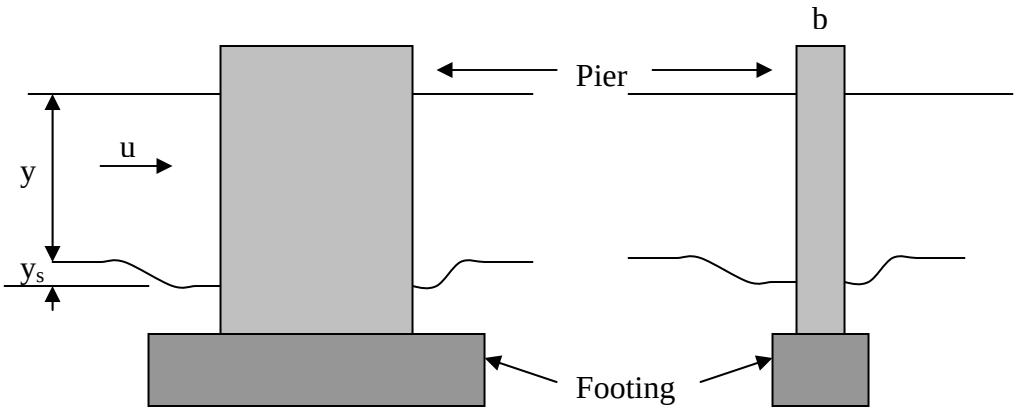

FIGURE 1. Definition sketch of pier scour

1.2 Scour Depth Estimation

The equilibrium scour depth, y_s, is expected to vary according to the characteristics of the approach flow, the bed material and the width of the pier. Here the shape and alignment of the pier, and the non-uniformity of the bed material are not considered. An analysis of these parameters results in the following (*1*);

$$\frac{y_s}{b} = f\left(\frac{u^2}{gy}, \frac{y}{b}, \frac{b}{d_{50}}\right) \qquad (1)$$

where d_{50} is a representative size or diameter of the bed material. Other parameters are defined in Figure 1. The complexity of the hydrodynamics associated with the turbulent flow around piers and the complications in predicting sediment transport led to the development of many empirical relations based on laboratory experiments and field data. Because of the inherent complexity of the field phenomena and the associated deficiencies such as sparsity and incompleteness of field data there is considerable uncertainty regarding the relative importance of various parameters. Scour prediction formulae include parameters such as depth of water, shape of the pier nose, speed and angle of attack of the approaching flow, width and length of the pier, bed condition (*2,3*). Scour prediction formulae recommended by HEC-18 are provided in Appendix.

In order to apply scour prediction models, the hydraulic, geometric and sediment parameters need to be measured in the field. The geometric parameters can be obtained from previous measurements and design plans for the bridge. Angle of attack of the approaching stream flow, water temperature and the sediment grain size data can be obtained from direct observations. Other important parameters common to pier-scour computations are the depth and velocity of streamline flow immediately upstream of a pier. Simple computation methods for maximum velocity as recommended by HEC-18 are summarized in Section 2. Observations have to be made to measure the current speed at locations and times of interest. Measurement of these parameters while simultaneously monitoring the scour will help in correlating the scour prediction models to actual observed scour. It should be noted that no such measurements were made during the present study.

1.3 Scour Monitoring Using Acoustic Instruments

Many types of fixed scour-monitoring devices are available for measurement of local scour around structure foundations *(4,5,6)*. An overview of the various types of fixed instruments is presented by Trent and Friedland (*7*). The Federal Highway Administration and other interested organizations have sponsored numerous research projects to identify the most accurate and dependable instruments for the scour monitoring. The most common types are various sonar instruments and mechanical sliding collar devices. Sonar systems were determined to be both accurate and dependable, and required the least maintenance. In addition, the installation of sonar systems with data storing capability allows for continuous scour monitoring (Lasa et al.(*8*)). In the following paragraphs three major acoustic instruments (echo sounder, side scan sonar and sub-bottom profiler) are described briefly.

An echo sounder determines water depth by repeatedly transmitting acoustic energy through the water column and recording the arrival time of the reflected energy from the water bottom. The time required for the signal to travel from its source to a reflector and back is known as the two-way travel time. The travel time of the acoustic pulse depends on the velocity of propagation in the water column. If the velocity of sound in the water column is known along with the distance between the reference water surface and the transducer, the corrected depth can be computed by the measured travel time of the pulse.

Most echo sounders use a narrow-bandwidth 200-kHz acoustic signal. This signal can be used to provide accurate depth data, but little or no information about the sub bottom. Echo sounders that use a lower frequency signal, such as 20 kHz, can detect reflected energy from sub bottom interfaces, such as the bottom of an unfilled scour hole. A class of wideband chirp echo sounders in the 1-10 kHz band have been used to image sub bottom layers (*1,9*). The chirp refers to the linear frequency modulation of the transmit signal.

Side scan sonar offers a high-resolution tool that provides a general depictive map on both sides of a survey vessel's path. Most side scan systems use transducers mounted on a tow fish pulled behind a survey vessel. The transducer in the tow fish emits an acoustic pulse that travels through the water and hits the bottom. The returning echoes are received by the transducers and processed to produce an image. The EdgeTech Subscan system which the Department of Ocean Engineering recently acquired is equipped with a side scan sonar. The details of this sonar are given in Section 1.3.

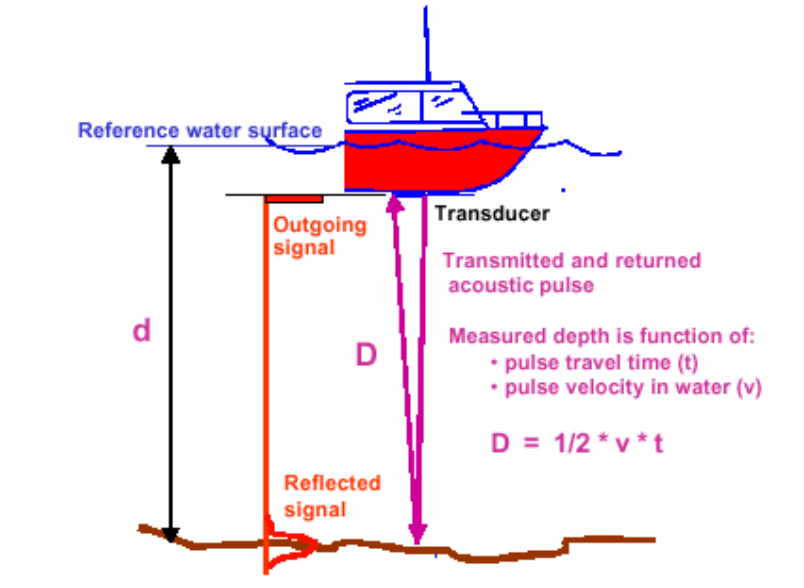

FIGURE 2. Acoustic measurement of depth (*10*).

A scour hole is generally thought to increase in depth on the rising limb of a flood, reaching a maximum depth at or near peak flow. As the flood recedes, however, the scour hole may be refilled by the upstream sediment transported after the peak flow is reached. This backfilling may mask the size of the scour hole, unless the bridge inspection is carried out during peak flood events (*1*). This leads to a gross under estimation of the scour if inspections are carried out during any other time period. Automated scour monitoring offers an alternative to periodic inspection wherein the maximum depth of scour at a fixed point is measured continuously over time, including during peak flood periods. It should be noted that fixed instruments do not provide the spatial extent of the scour unless multiple instruments are used. Also, if they are not installed at the location where maximum (over a region) scour occurs, which may conceivably vary with hydraulic conditions, their readings may underestimate scour. There are also variety of outside influences that may interrupt or terminate the data collection process. These include physical damage caused by debris and ice floating in water, lighting strikes and vandalism (*1*).

A useful tool for "looking through" the backfilled material in the scoured area is a sub-bottom profiler. The ability of a sub-bottom profiler to penetrate these recent deposits and delineate the full extent of historic scour enables accurate surveys to be conducted under more favorable conditions. In operation, a sub-bottom profiling system produces a real-time vertical profile of the riverbed. If present, the recent backfill material can be identified above the deeper scour holes. The basic system consists of a transmitter, receiver, graphic recorder and a set of transducers. The transmitter generates a high-power, low frequency signal to drive the underwater transducers. The transducer converts the electrical signal from the transmitter into

acoustic energy directing it towards the riverbed. At the river bed the acoustical energy travels downwards and encounters different layers of sediment. Some of the energy is reflected off these sediment interfaces while the remaining energy continuous downwards. The transducer picks up the reflected signals and it is amplified, filtered and displayed. This system can be easily deployed and operated aboard small vessels. Typically these systems give a penetration depth of 20 ft which is adequate for bridge scour surveys.

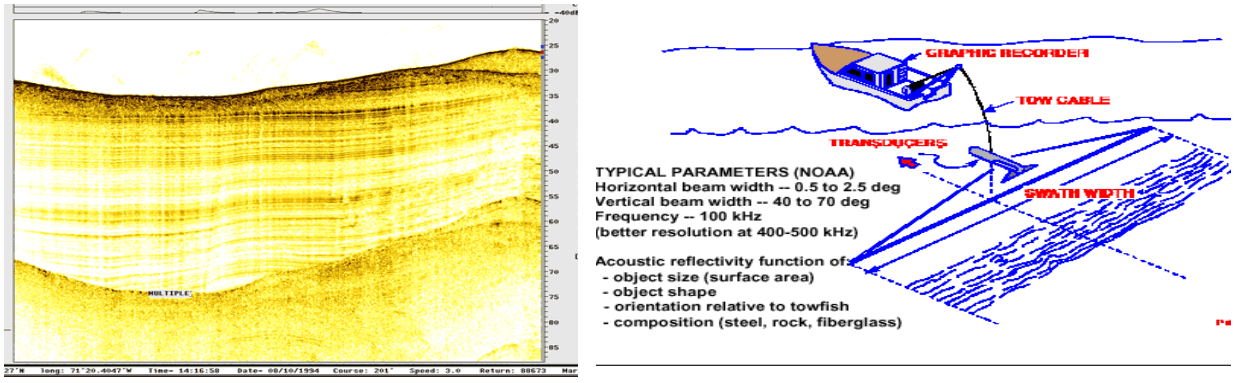

FIGURE 3. Sub-Bottom profiler image at a location in Narragansett Bay, RI using an X-STAR System, and SB-0512 transmitter (left panel). The acoustic reflectors show the layering in the sediment. This data was collected by EdgeTech.Side scan sonar (*9*). The right panel shows a side scan sonar (*9*).

1.4 The Integrated Side Scan Sonar and Sub-bottom Profiler

The Edgetech Subscan System provides the Department of Ocean Engineering a unique capability to undertake the present study. The EdgeTech side scan sonar is a versatile dual frequency system that provides an image of the bottom with ranges out beyond 500 m each side. One frequency is centered around 100 kHz and the other around 400 kHz. This side scan sonar is designed to work with the sub-bottom profiler. This system has been used for various applications including scour/erosion surveys in rivers and streams (*11*).

The EdgeTech Full Spectrum Sonar is a versatile wide band Frequency Modulated (FM) sub-bottom profiler that generates cross-sectional images of the seabed and collects normal incidence reflection data over many frequency ranges. A typical image taken using this system is shown in Figure 3. This system has several advantages over conventional sub-bottom systems, including increased penetration and higher resolution. The frequency range of operation is determined by the acoustic characteristics of the transmitter and receiver mounted on the tow vehicle. The frequency range is typically 2-16 kHz. Each vehicle can transmit acoustic pulses with different center frequencies and bandwidths. The selection of the pulse is made on-line by the operator while profiling to achieve the best imagery. The towed vehicle is selected based on the sub-bottom conditions at the survey site and the type of sub-bottom features that need to be imaged. The vertical resolution is in the range 6 to 10 cm depending on the pulse bandwidth used. The penetration is typically 10 m in calcareous sand and 80 m in soft clay (*11*).

1.5 Sidescan Sonar and Sub-bottom Profiler Principles

Sections 1.2 and 1.3 provide the basic introduction into the sidescan sonar and sub-bottom profiler. This Section presents, in more detail, the applications of these instruments for sediment classification and scour detection. Two examples from published literature are provided

to highlight the usefulness of these instruments. Side scan sonar instruments are towed behind ships and often called towfish or tow vehicles. The instrument sends out a sonar signal in pulses at right angles to the direction the ship is moving (so it is "looking" sideways and down). The sonar signal is concentrated in a narrow band on both sides of the tow vehicle. Some of the sound sent out by the side scan sonar reflects off the seafloor and returns to the tow vehicle. The tow vehicle has sensitive hydrophones (also called receivers) which receive the returning sound. The signals from the hydrophone are sent to the ship for processing and an image is made showing the strength of the returned sound over the area the tow vehicle was sending the sound. High backscatter (low signal attenuation) surfaces are generally coarse sediments and/or exposed rock or other hard bottom material and low backscatter (high signal attenuation) surfaces are generally fine sediments. Also a strong return received if the seafloor slopes slops towards the instrument. Any feature that rise above the surrounding seafloor will cast acoustic shadows.

Sidescan-sonar data represent backscatter received by the sidescan-sonar tow vehicle from an insonified region of sea-floor. Acoustic backscatter is thought to be a function of the angle of incidence of the acoustic wavefront to the sea-floor, surface roughness, and impedance contrast across the sediment-water interface, topography, and volume reverberation (Urick (*12*)). The strength of the sound recorded by the instrument is then converted into shades of gray (in gray scale images). Within digital sidescan-sonar imagery, high backscatter is represented by light tones, low backscatter by dark tones (Figure 4). In general, areas of high backscatter are associated with relatively coarser-grained sediments, areas of low-backscatter with relatively finer-grained sediments. However to accurately interpret the geology of an area correlations must be made between the surficial sediment characteristics acquired by sidescan-sonar and groundtruth techniques, and the underlying structure acquired through use of seismic reflection techniques.

Figure 4 is a schematic showing the sidescan sonar in operation and the sonar back-scatter output. The intensity of sound received by the sidescan-sonar tow vehicle from the sea floor (backscatter) provides information as to the general distribution and characteristics of the surficial sediment. Strong reflections (high backscatter) from boulders, gravel and vertical features facing the sonar transducers are shown white; weak reflections (low backscatter) from finer sediments or shadows behind positive topographic features are shown black.

Figures 5 and 6 illustrates the capabilities of the sidescan sonar in determining sediment types and bridge pier scour. Figure 5 display a geologic interpretation of the New York Bight Apex overlain on sidescan-sonar imagery (*13*). This interpretation was based on analysis of sidescan-sonar, sedimentologic and subbottom data. Figure 5 shows the surficial sediment distribution. The different colors represent different sediment types with different backscattering strength. Side scan sonar provides a map of the bottom on both sides of a towing vessel. Sub-bottom profiler- provides a vertical profile of the seabed. Ability to ‘look through’ the backfilled material in the scoured area makes it very useful for scour monitoring.

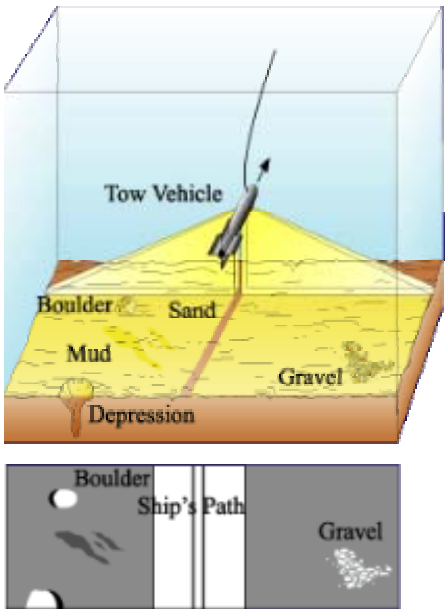

FIGURE 4. Schematic showing the sidescan sonar in operation and the sonar back-scatter.

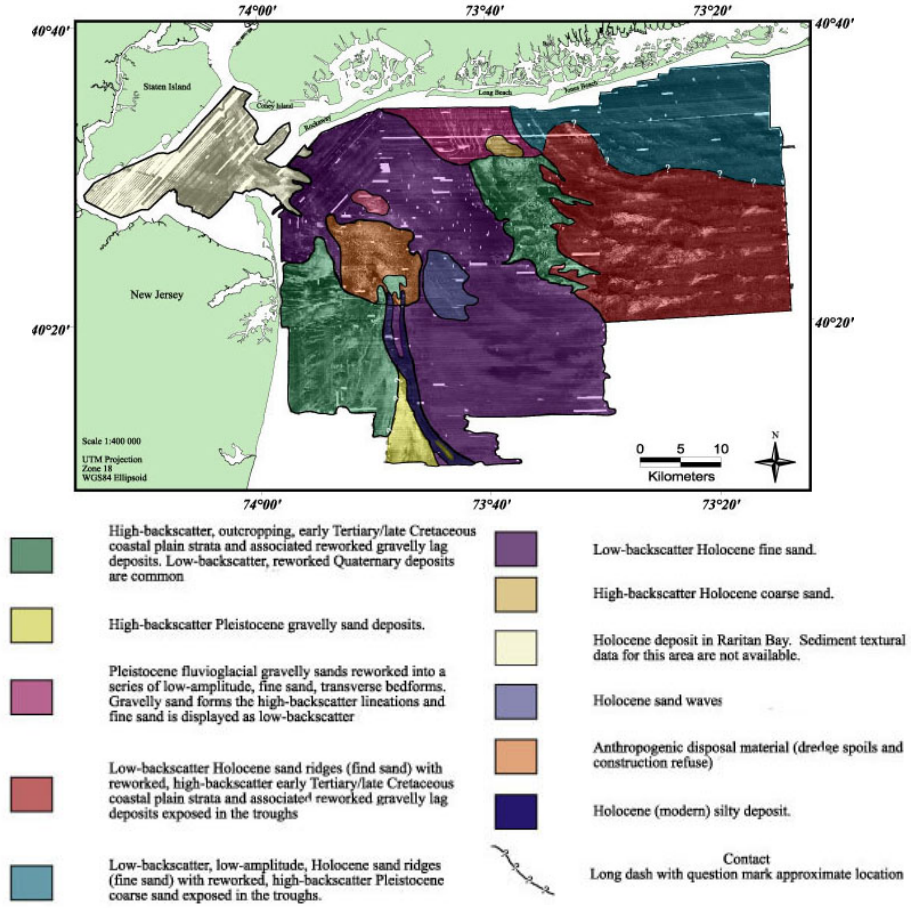

FIGURE 5. Sidescan sonar imagery collected within the New York Bight Apex and geologic interpretation. The different colors represent various sediment types with different backscattering strength.

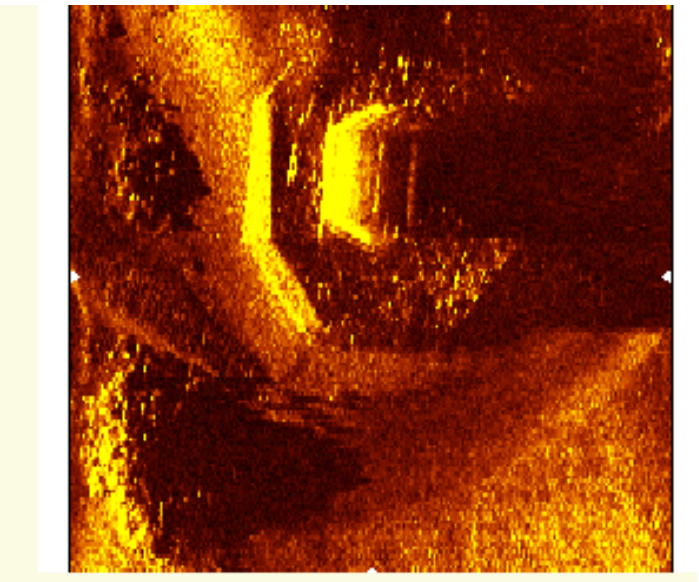

FIGURE 6. Side scan image showing evidence of scour around a bridge pier in Alton, IL (*14*).

Figure 6 shows an example where sidescan image clearly shows the presence of scour around a bridge pier in Alton. IL. The horizontal extent of the scour can be visualized comparing it with the dimensions of the pier footing. The horizontal dimensions of the scour hole seem to be comparable to the dimensions of the footing in this case.

2.0 SCOUR ANALYSIS FOR TIDAL AREAS

In the coastal region, scour at bridges over tidal waterways that are subjected to the effects of astronomical tides and storm surges is a combination of long-term degradation, contraction scour, local scour and water way instability. Although many of the flow conditions are different in a tidal waterway compared to a riverine system the local scour can be estimated using the same set of equations (Appendix) if the hydraulic condition (depth, discharge, velocity etc.) is carefully evaluated. The continuous rise and fall of astronomical tides will usually influence long-term trends of aggradation or degradation. Conversely when storm surges and tsunamis are a single event phenomenon which, due to their magnitude, can present a significant threat to a bridge crossing in terms of scour. Other factors which may affect the scour process are;

1. Littoral drift – transport of beach material along the coast resulting from wave action. This littoral transport of sediment serves as a source of sediment supply to the inlet, bay or estuary, or tidal passage.
2. Mass density stratification can result in larger velocities near the bottom than the average velocity in the vertical.
3. Salinity can affect the transport of silts and clays by causing them to flocculate and possibly deposit.

Evaluation of Hydraulic Characteristics

The velocity of flow, depth, and discharge at the bridge waterway are the most significant variables for evaluating bridge scour in tidal waterways. Direct measurements of the value of these variables for design storm are rarely available. These parameters are often estimated using coastal engineering models and equations. Physical models or the use of sophisticated computer models can be employed for this purpose. Alternatively, either a procedure by Neil (*3*) for

unconstrained water ways or an orifice equation for constrained tidal inlets can be used to evaluate the hydraulic conditions at bridges influenced by tidal flows. Extreme events associated with floods and storm surges should be used to determine the hydraulics at the bridge to evaluate local or contraction scour.

The Narragansett Bay system is a complex shallow water system, having two large water bodies, Narragansett Bay and Mount Hope Bay, at the center of the system. The two bays are connected to two major rivers to the north, the Providence River and Taunton River, and join the East and West Passages and the Sakonnet River to the south. The whole system eventually unites the Rhode Island Sound to the south. Newport Bridge spans across the Narragansett bay. The Sakonnet River is located between Mount Hope Bay and Rhode Island Sound, transferring tidal energy between the two areas. The volume of the river is 3 km (width) × 20.5 km (length) ×10 m (mean low water, MLW, depth) and the surface is approximately one-sixth of the Narragansett Bay system. The River consists of two parts, the lower and upper section. The former is of a rectangular shape, 2.6 km width by 18 km length. The latter is shaped as a sand timer with two bottlenecks produced by causeways at the Railroad Bridge (north) and Old Bridge (south). The length of the upper section is only about one-fifth of the lower. The depth-averaged, north-south velocity components at the Railroad Bridge speed vary between –2 m/s and 2 m/s (Kim and Swanson (*15*)). From RIEMA (*16*), the storm surge tidal range at Narragansett corresponds to the two hurricane events in 1938 and 1954. The values reported for these two events were 13.7 ft (4.1758 m) and 14.4 ft (4.3891 m) referenced to MSL.

Neil (*3*) has developed an approximate equation to determine the maximum discharge in an ideal estuary using the following equation

$$Q_{\max} = \frac{3.14 Volume}{T} \qquad (2)$$

Q_{max}=Maximum discharge in the tidal cycle, m^3/s
Volume= Volume of water in the tidal prism between high and low tide levels, m^3
T- Tidal period between successive high and low tides, s

A simplification of the above equation, suggested by Chang (*3*), is to assume the tidal prism has vertical sides. With this assumption above equation becomes

$$Q_{\max} = \frac{3.14 A_s H}{T} \qquad (3)$$

A_s=Surface area of the tidal prism at mean tide elevation, m^2
H- Distance between successive high or low tides.

The corresponding maximum (depth averaged) velocity (V_{max}) in the waterway is:

$$V_{\max} = \frac{Q_{\max}}{A_c} \text{ m/s} \qquad (4)$$

A_c = Cross sectional area of the waterway at mean tide elevation, m^2

The scour at the crossing can be computed using the values of the discharge, velocity and depths determined from the above analysis and the scour equations summarized in the Appendix. For the Sakonnet river bridge, if we substitute RIEMA storm surge tidal range (1954 hurricane), the approximate area of the tidal prism, a tidal period of 24 hrs and the area of water way from the cross-section (left panel, Figure 7) we get a maximum velocity, due to storm surge, of

approximately 0.5 m/s. Using these values for velocity, a pier width of 5 m and the water depth from the depth sounder recordings in Equation A1 we can come up with a scour depth of approximately 7.0 m. Hence the top width of the scour hole will be of the order of 15 m assuming cohesionless soil and using Equation A5.

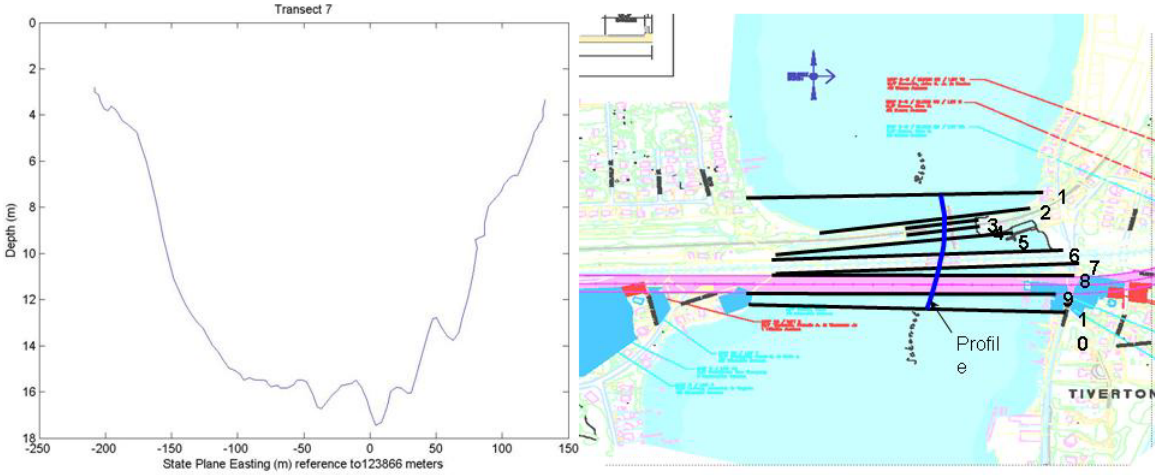

FIGURE 7. Depth cross section for transect 7 (left panel). The location of the transect is shown in the right panel.

3.0 FIELD EXPERIMENTS

Two field experiments were conducted in which the Sidescan Sonar and Sub-bottom profiler were deployed. The first field experiment was conducted in October, 2003 near the Newport Bridge. Sidescan sonar and sub-bottom profiler were deployed from the research vessel R/V CT-1 in this cruise. The second field test was conducted in April, 2004 near the Sakkonet river bridge. Another research vessel, R/V Quest, was used to deploy the sonars in this cruise. The Newport bridge spans across the Narragansett Bay and the primary source of energy inducing erosion and scour in this case are tidally driven currents. The highway bridge at Sakonnet spans the Sakonnet River and in this case also strong currents due to tidal action are predominant. The field work was carried out during low currents for better maneuvering capabilities. Hence no direct measurements of the peak currents were made during these experiments. But predictions and measurements of currents are available in literature which can be used in the empirical scour prediction formulae to compute the scour in this study. Major emphasis in this study is given to identification of the scour problem and the horizontal extent of it. The comparison of the scour depth with predicted values is difficult as the computation of scour depth requires environmental, sediment and geometrical parameters, the collection of which may require additional field efforts.

3.1 Newport Bridge Field Study

Side scan sonar and sub-bottom profiler were deployed near the Newport Bridge in October, 2003. This Section describes some of the images acquired during this survey. The top panel in Figure 8 shows the location of the field test and the survey tracks which go around the bridge piers which are labeled in the bottom panel. The maximum water depth in the channel is approximately 130 m as shown in the figure. The sidescan sonar was deployed from the R/V CT-1 and the sonar provided images of the condition of bridge piers. Few images, in which evidence of scour is very prominent, are shown in Figures 9 to 15. Figure 9 to 12 shows the sidescan images of looking from the four sides of Pier A (see Figure 8 for pier notations). The left and

right panels show the images of the same location with different resolution (using different frequencies).

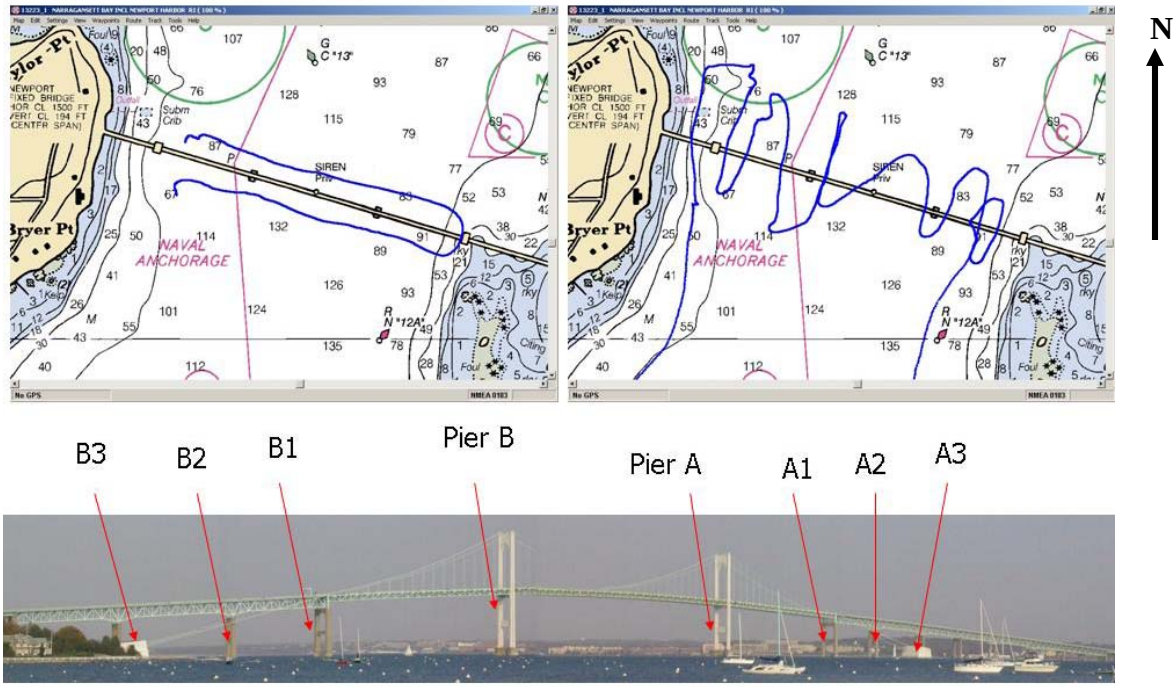

FIGURE 8. The tracks surveyed during the field test in Newport. The tracks are chosen to cover all the sides of the piers. The top two panels show the tracks and the bottom panel shows a picture of the Newport Bridge with the piers numbered for further reference.

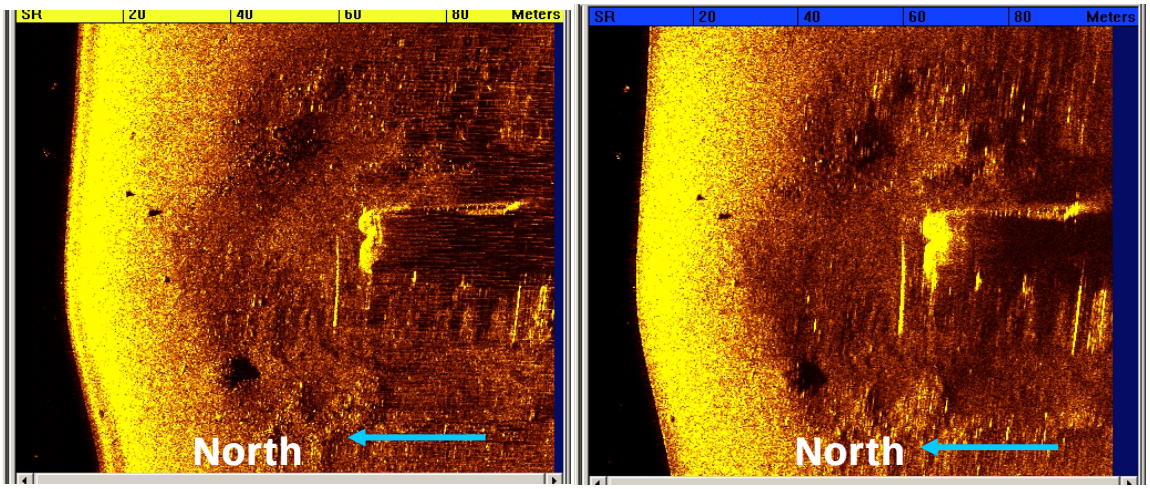

FIGURE 9. Sidescan images of pier A. The two images show the same location at two different resolutions (the two images were acquired using two frequencies). The position of pier A is shown in Figure 8.

Figure 9 shows substantial scour hole around the pier A. The width of the scour depression, as read from the scale at the top of the image, is of the order of 40 m. This is large

compared to the size of the pier as can be seen from the figure. We can also see some other features resembling the exposed edges of pier footings. Figure 10 shows the southern side of the pier A. A large depression resembling a scour hole is clearly visible in the image. The exposed edge of the footing is also visible in this image. The horizontal extent is comparable to the northern side of the pier as seen in Figure 9.

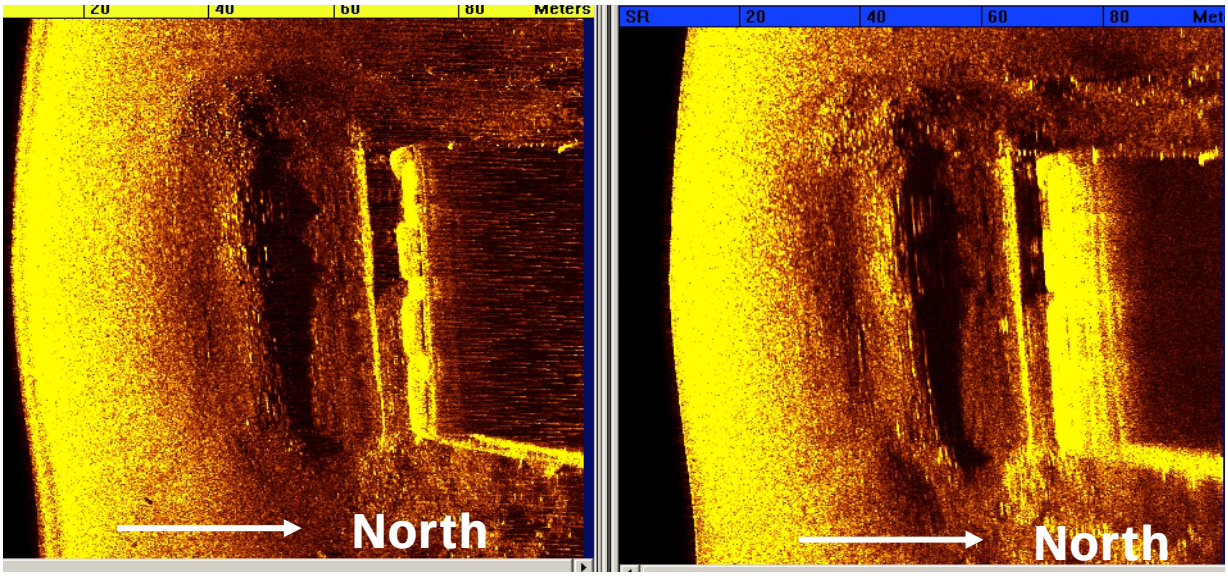

FIGURE 10. Sidescan images of pier A. The two images show the same location at two different resolutions (the two images were acquired using two frequencies).

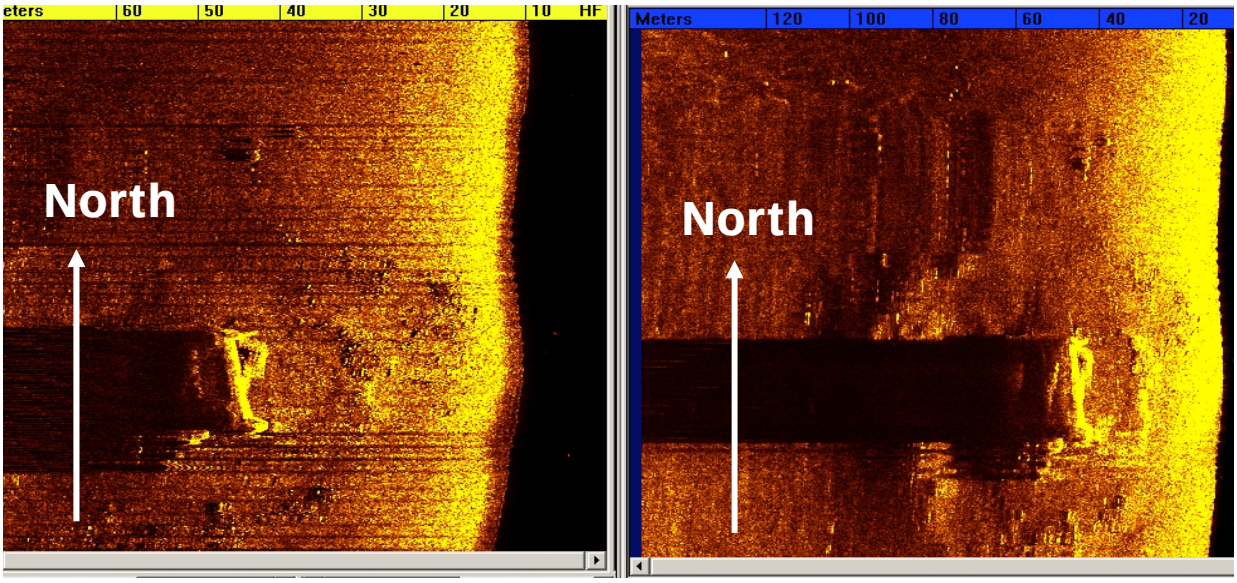

FIGURE 11. Sidescan images of pier A. The two images show the same location at two different resolutions (the two images were acquired using two frequencies). Note that the scale (top of the figures) is different in the two panels.

Figure 11 shows the western side of pier A. A large depression can be seen on this side also with horizontal dimensions of the order of 20 m. Compared to the other sides the horizontal extent of the scour seems to be less. Figure 12 shows the image of Pier A with very low scour on the eastern side. It should be noted that in Figure 11 and Figure 12 the scale of the images are different for the left and right panels. Figure 12 also shows an interesting feature on the eastern side. This feature with linear dimensions of the order of approximately 15 m can be seen in both the panels, even though it more clear in the left panel. It appears like an exposed reinforcing bar or debris near the pier. Overall, it can be seen that Pier A has been affected with scour with the extent of scour different on each sides.

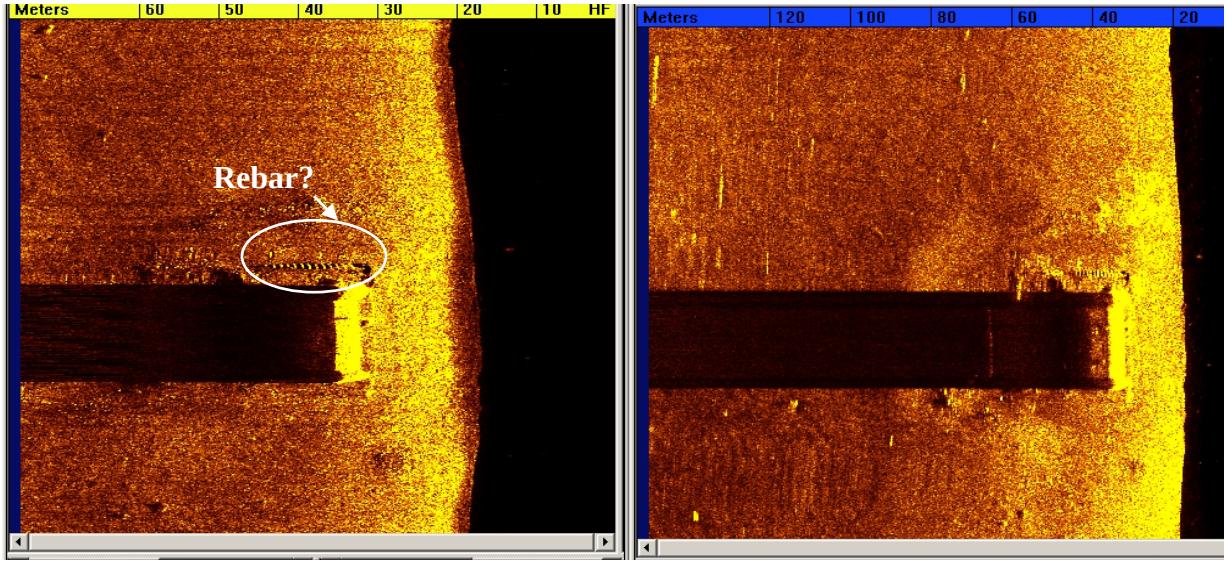

FIGURE 12. Sidescan images of pier A. The two images show the same location at two different resolutions (the two images were acquired using two frequencies).

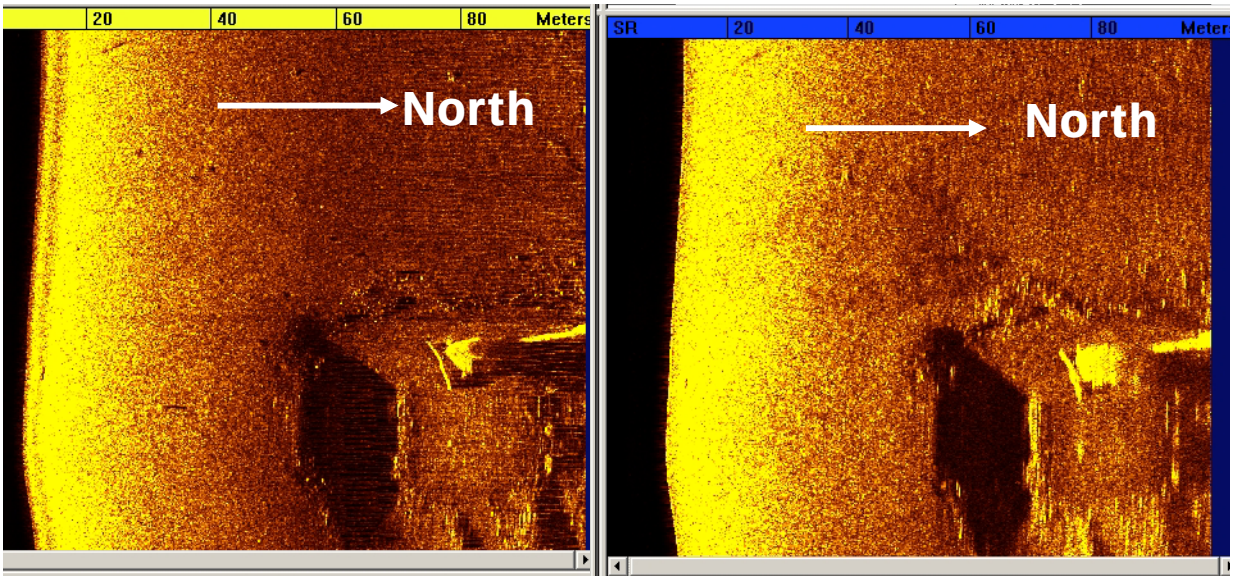

FIGURE 13. Sidescan images of pier A2. The two images show the same location at two different resolutions (the two images were acquired using two frequencies.

Figure 13 shows the image of the southern side of Pier A2. A big scour hole is visible on the southern side with north-size dimension of the order of 20 m and east-west dimension 40 m. We can also see some disturbance on the east and west sides even though they are not comparable to the one in the south side.

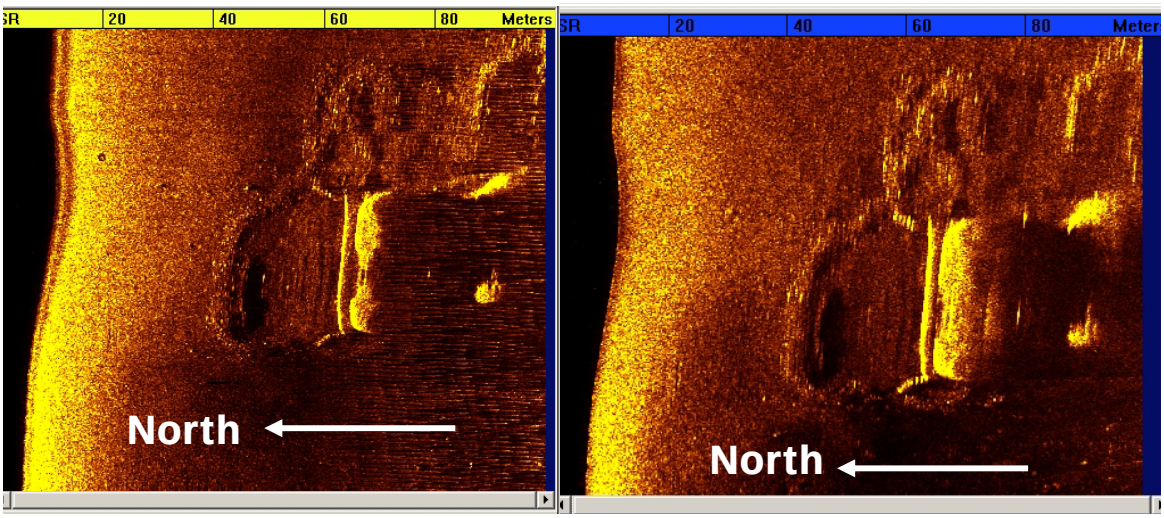

FIGURE 14. Sidescan images of pier B2. The two images show the same location at two different resolutions (the two images were acquired using two frequencies).

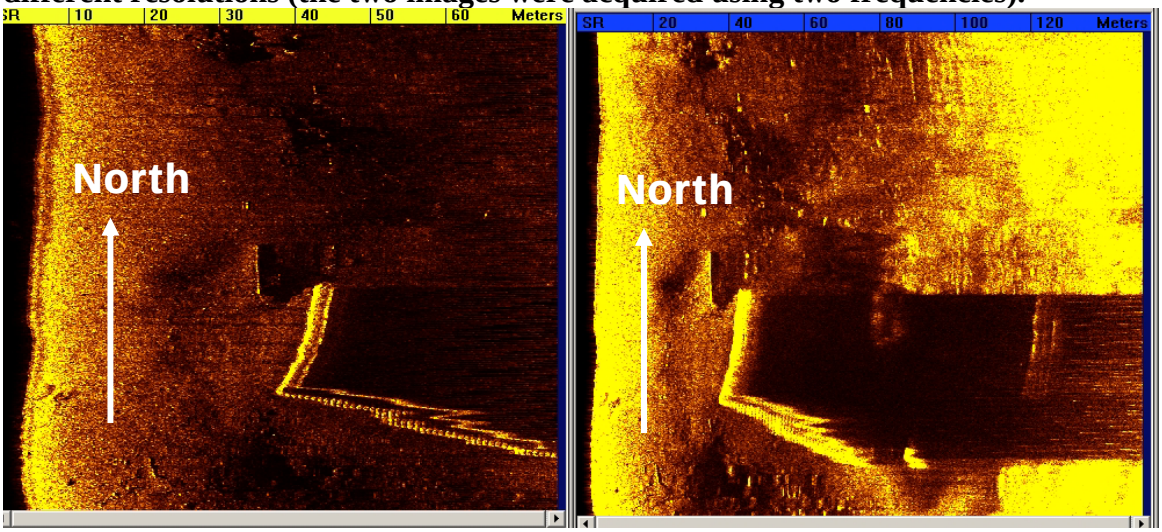

FIGURE 15. Sidescan images of pier B3. The two images show the same location at two different resolutions (the two images were acquired using two frequencies).

Figures 14 and 15 show the side scan images around two smaller piers (B2 and B3) which are closer to the land. Figure 14 shows large disturbances in the sediment near B2 on the northern and western sides of the pier. Similar depressions can also be seen around pier B3 also. We can see another feature near the pier B3, on the north-west corner of the pier, which appears to be part of the pier sub-base or debris near the pier.

The side-scan images of other bridges were similar in nature with varying amounts of scour around the piers. The sub-bottom profiler also produced profiles of the sediment structure

near the piers. Figure 16 shows an image produced by the sub-bottom profiler showing the different sediment layers present near the bridge. There seems to be a major reflector corresponding to a 5 meter surface layer and some minor reflectors at various depths. The 5 m top layer may be redeposited material but no additional information is available at present to validate this hypothesis.

Encouraged by the success of the first field experiment, whose main objective was to test the equipment and to get experience in towing the fish around bridge piers in the presence of large currents, another field experiment was conducted in a much shallower location in Sakonnet. The following section provides more details of this field test.

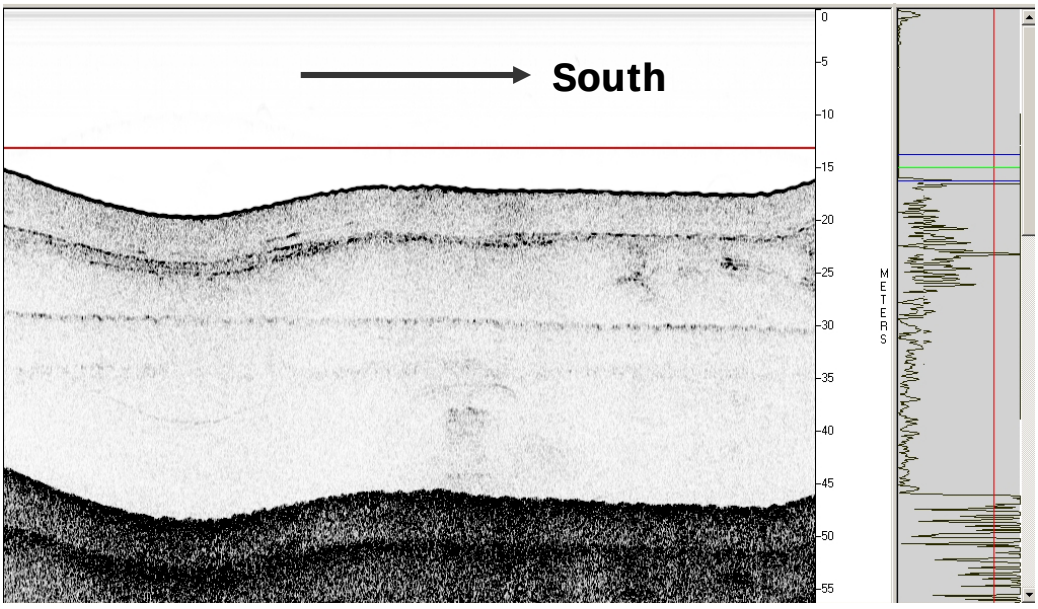

FIGURE 16. Sub-bottom profile near pier A1.

3.2 Sakonnet River Bridge Field Test

The sidescan sonar- subbottom profiler system was deployed from the research vessel R/V Quest near the Sakonnet river bridge on April 20, 2004. The location of the field deployment is shown in Figure 17. The objective was again to detect the presence of scour around the highway bridge piers. The water depth at this location, approximately 17 m, is much less than the previous study area. The deployment was difficult in this site due to the lower water depth, high currents, presence of many fishing boats, presence of the railroad bridge, and the presence of a drilling barge anchored close to one of the piers. All this factors made the maneuvering of the research vessel and the tow fish very difficult. The barge and its anchor lines prevented easy access for the sonar around one of the piers. In spite of this challenging environment sonar was able to obtain images of the other piers.

The survey was carried out in such a way that the sonar could capture images of the bridge piers from all sides. The water depth decreases rapidly towards the riverbanks on either side and hence the outer piers were hard to image. In addition to the sidescan-subbottom system we also operated a depth sounder continuously. The depth sounder data was logged concurrently with the GPS data using a multiplexer. The depth sounder data was then used to produce a bathymetry map of the area adjacent to the highway bridge (Figure 18). The main channel seems to be 15 to 17 m deep (below the Mean Lower Low water level) and shallower near the edges

(~2 m). Width of the water way near the bridge is of the order of 400 m (Figure 7). The sonar images were then processed to identify the presence of any scour around the concrete piers. The sonar images of the bridge piers indicate the presence of scour and also show debris and sand ripples (Figure 20-24).

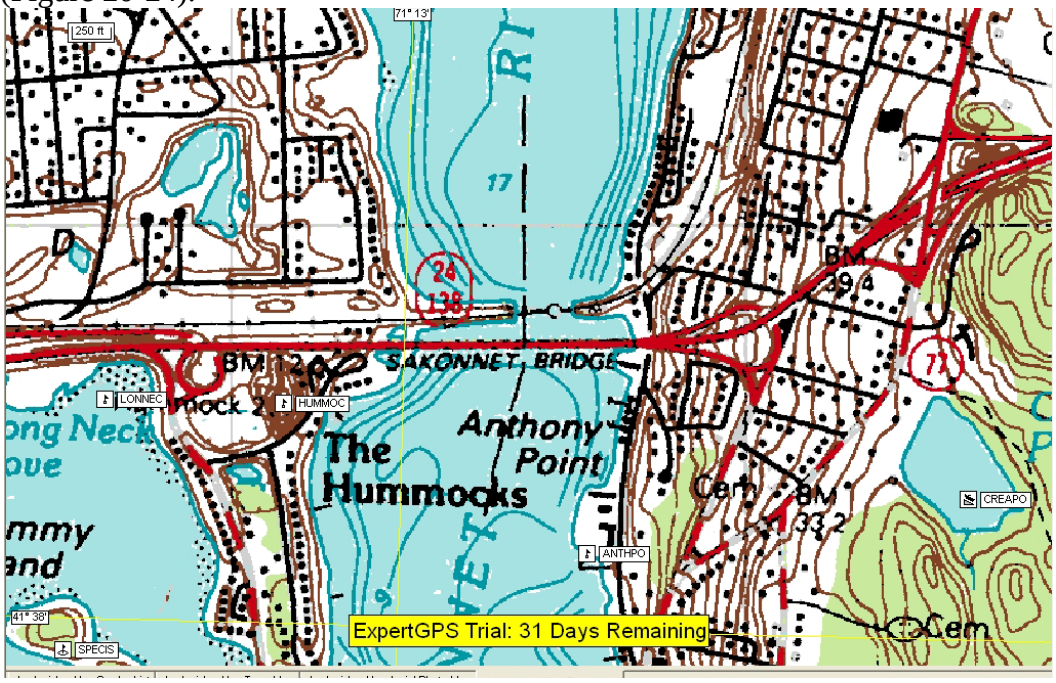

FIGURE 17. Location of the sidescan survey at Sakonnet. The highway bridge and the railroad crossing can be seen in this figure.

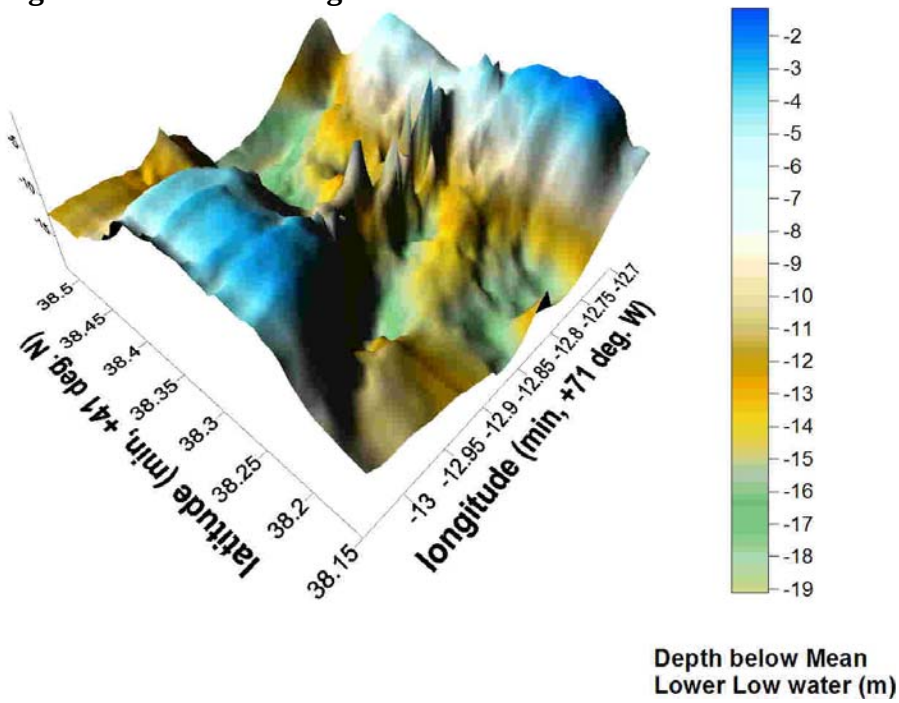

FIGURE 18. Bathymetry map of the area adjacent to the Sakonnet river bridge.

FIGURE 19. View of the highway bridge at Sakonnet with piers marked as A, B and D. The drilling barge (near B) and the old railroad bridge can also be seen in the picture.

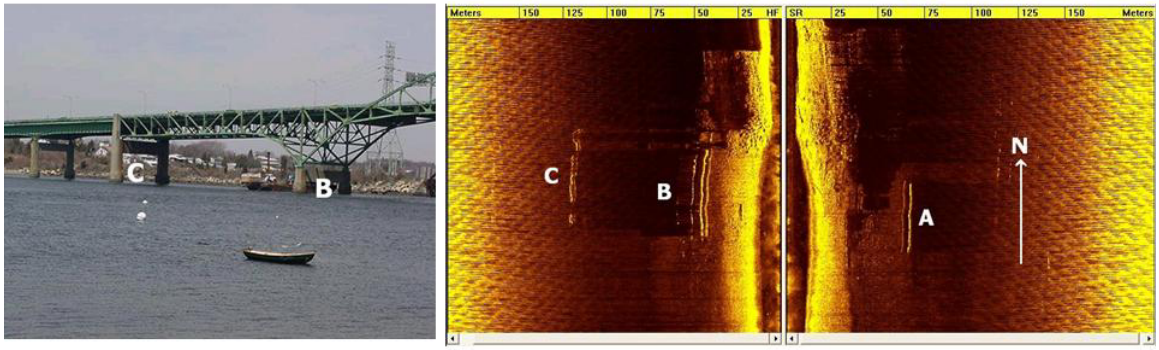

FIGURE 20. View of the bridge piers. Right panel shows the side scan sonar image near pier B and C.

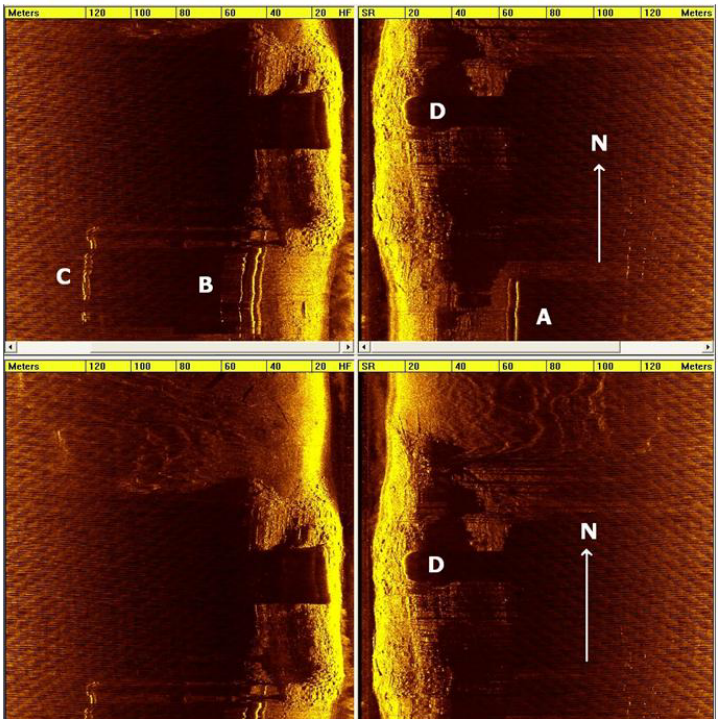

FIGURE 21. High frequency Sidescan images of the bridge pier at Sakonnet.

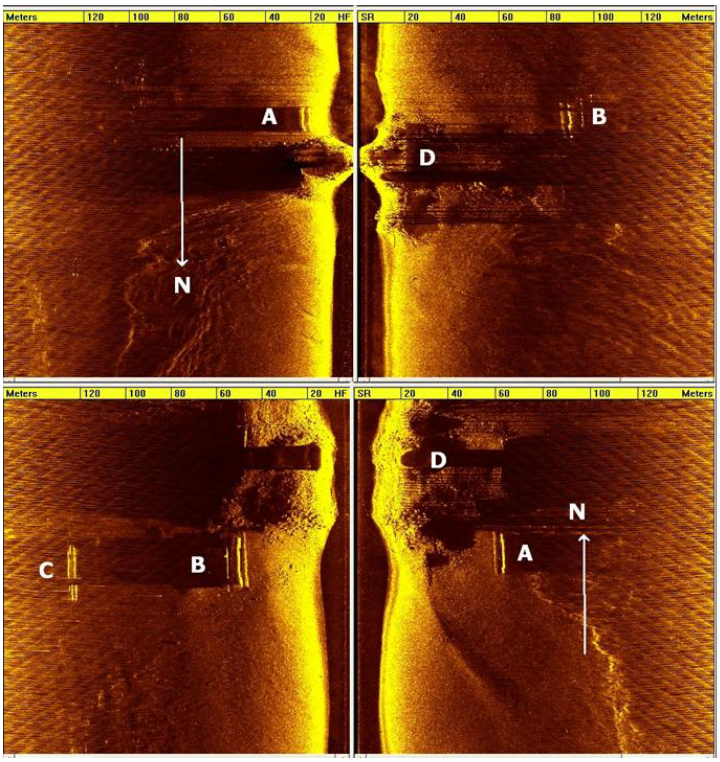

FIGURE 22. Sidescan image of the bridge pier at Sakonnet. Both the upper and lower panels show high frequency images (high resolution).

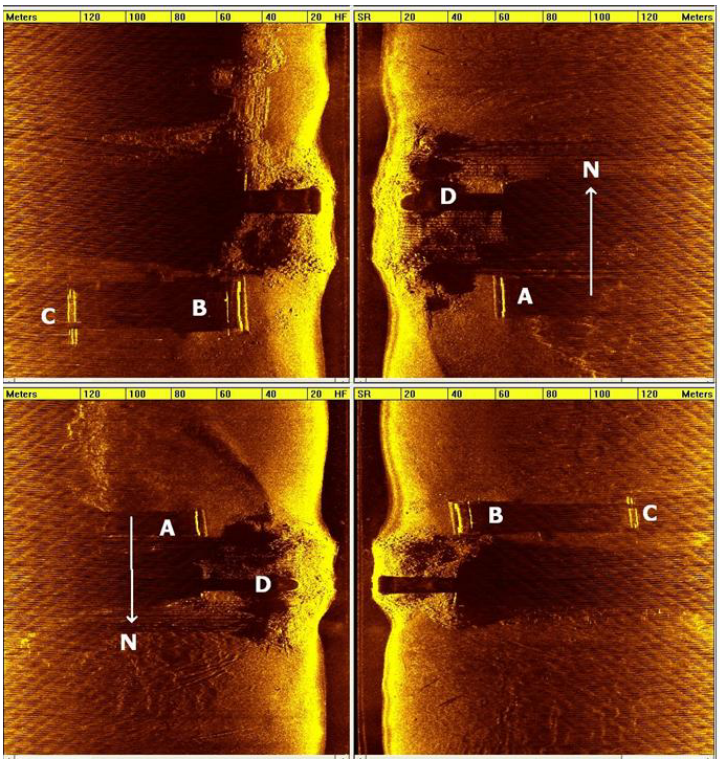

FIGURE 23. Sidescan image of the bridge pier at Sakonnet. Both the upper and lower panels show high frequency images (high resolution).

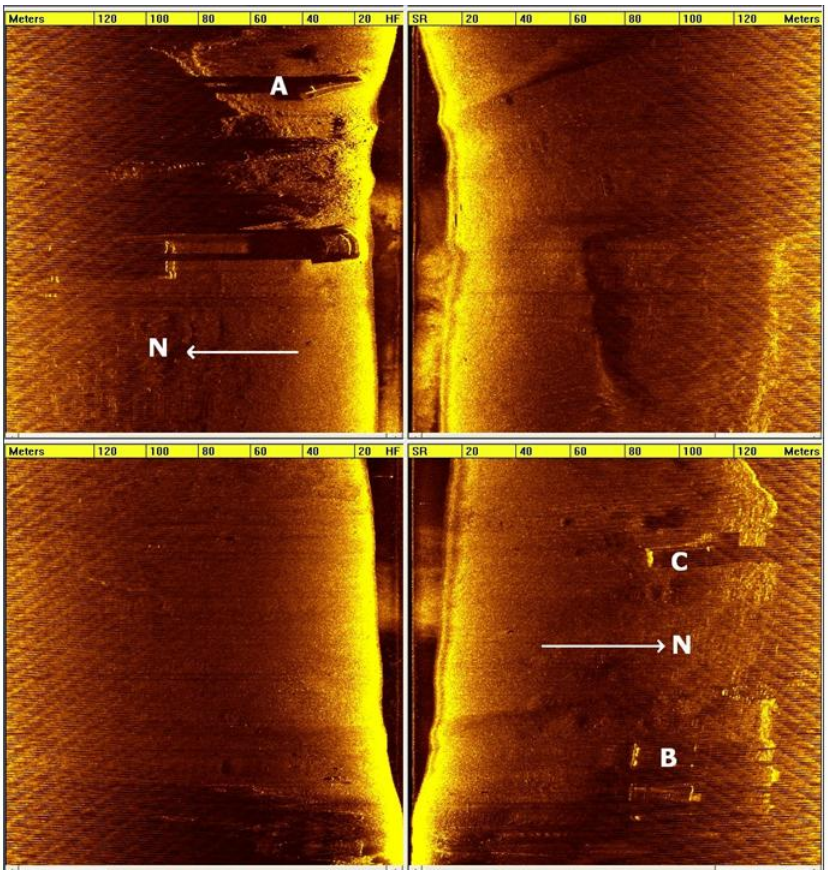

FIGURE 24. Sidescan image of the bridge pier at Sakonnet. Both the upper and lower panels show high frequency images (high resolution).

Left and Right panels in Figure 19 and Left panel in Figure 20 show the locations of the bridge piers whose side scan images are shown in Figures 20-24. The barge which was anchored close to Pier B can be seen in the right panel of Figure 19 and left panel in Figure 20. The main waterway (deepest portion of the channel) is between piers A and B. Pier C is in much shallower part of water. The quality of the sidescan images are not as good as the ones shown for Newport Bridge in Section 3.1. This can be attributed to the difficulty in navigating the boat and towfish close to the piers due to shallow water, high currents, and the presence of the barge with its anchor lines near Pier B.

In spite of the difficult operating conditions the sonar images provide evidence of areas of disturbances near the bridge piers which may be scour related. North-east side of pier B shows a large area of disturbance in sediment approximately 25 m in width (east-west direction) in Figure 20 (Right panel). From the top and bottom panels of Figure 21 it can be seen that this feature is approximately 100 m long (north-south direction). Another affected area is pier D as can be seen in Figures 21, 22 and 23. The horizontal dimensions of this feature near pier D (40 m in width and 110 m in length) are comparable to the one near Pier B. The area near Pier A is shown in the lower panel in Figure 23 and upper panel in Figure 24. The disturbances in soil due to scour are not visible as clearly as in the case of Pier B and D. A channel like depression, 50 m wide, can be seen in Figure 23. The information provided by these images is very valuable considering the fact that no *a priori* information was available at the time of the survey. Hence close

investigation of affected areas was not possible at the time of this study. Now that this information is available, any future study can concentrate on these areas that were shown to be affected in this survey. Hence as a first look at the bottom sediment scour this study provided valuable information and can be considered as a successful application of side scan sonar.

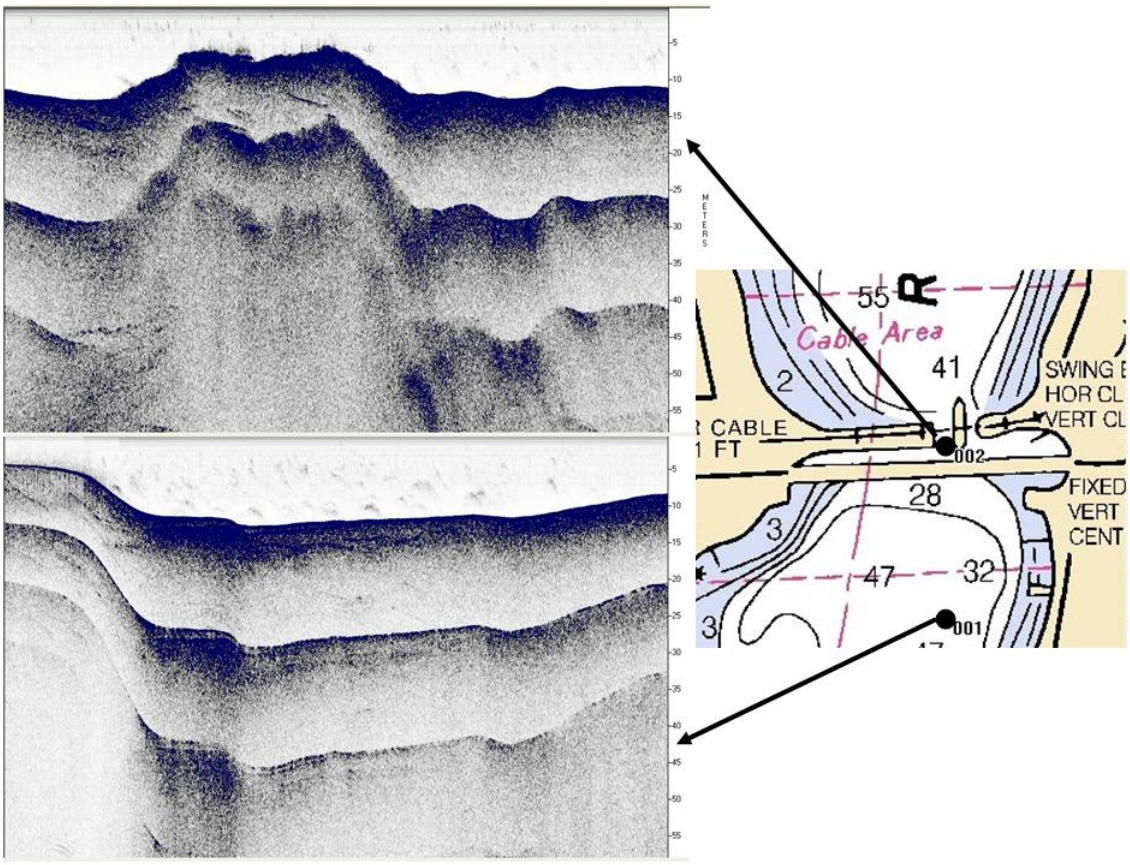

FIGURE 25. Sediment layers observed by the sub-bottom profiler. The top image is from a location close to the bridge pier and the bottom image shows a location far away from the bridge. The locations are marked in the right panel.

Figure 25 shows a comparison of the sediment layers at two locations: one close to the bridge pier and the other far away from it. Near the bridge we can see a shallow bottom with some layers in sediment. Since this is a localized feature it may be caused by erosion/deposition in the affected area.

4.0 DISCUSSION AND FUTURE WORK

The major objective for this study was to explore the possibility of using underwater acoustic instruments to detect or monitor the occurrence of scour around bridge piers. The study also investigated the possibility of estimating the extent of scour. Two field experiments at highway bridges in Newport and Sakonnet River, were conducted in October, 2003 and April, 2004 respectively. Each of these field test lasted one day and were conducted aboard R/V CT-1 and R/V Quest respectively. The EdgeTech sidescan sonar was used to get 2-D images of the bottom around bridge piers. Significant amount of scour was observed in the side scan images at both sites. The EdgeTech system has a sub-bottom profiler capable of looking through the

sediment to produce profiles of the sediment. This will give the thickness of layers of the sediment. This has the capability of detecting sediments with different properties. This then has the potential of detecting deep scour holes filled with sediment re-deposition. This will be possible since the refilled material will have different properties compared to the original (surrounding) material.

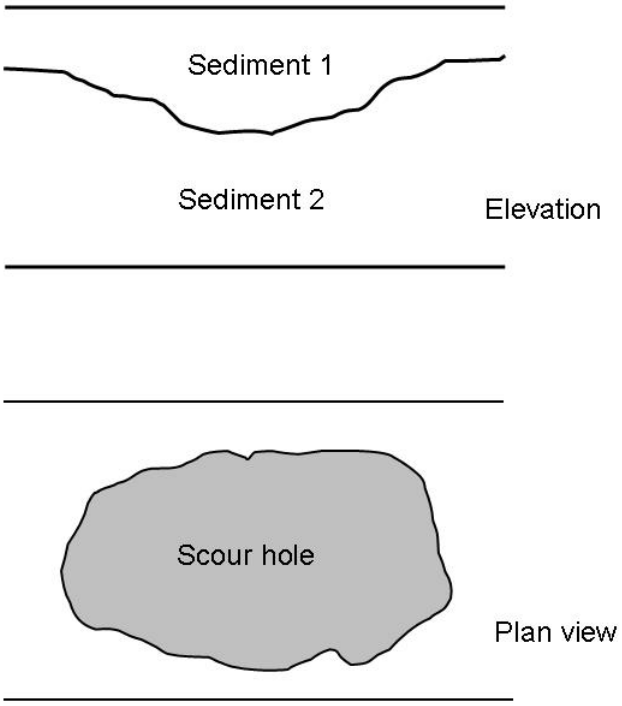

FIGURE 26. A schematic representation of a scour hole re-filled with new sediments. Sub-bottom profiler can be used to identify these two sediment types.

The major outcomes of this study can be summarized as follows:

1. As a detection/ monitoring tool, the deployment of sonar was successful. As can been seen from the sidescan sonar images the presence of scour around bridge piers at both locations was observed. Periodical survey of the same location will provide a tool for monitoring the growth, if any, of these scour holes. The surveys can be timed to monitor the effects of big storm events. The side scan survey will also provide the presence of any debris or other material around the bridge piers. If the piers are protected against scour (using boulders, concrete blocks etc.) the side scan images will be able to verify whether they are still in place or displaced. The sidescan surveys will provide an excellent tool for detecting and monitoring the bridge pier foundations.
2. The use of sub-bottom profiler for estimating the extent of scour is possible in severely affected areas (with large in-filled scour holes). A comparison of profiles produced by the sub-bottom profiler close to the bridge pier and away from it will provide different layering of sediments if the bridge pier is affected by scour. The sub-bottom profiler looks directly downwards and it is very difficult to tow the fish very close to the piers. Hence it is very difficult to get profiles close to the bridge piers. High currents, shallow water and presence of other vessels will further complicate the survey. All these factors were present at Sakonnet making the towing of the fish very difficult. Hence we couldn't thoroughly test this hypothesis. But the sub-bottom profiles look promising making this a

possible application. A combination of sidescan and sub-bottom profiler images should provide an estimate of the scour hole in 3-D. In Figure 26, the sub-bottom profile will provide an image similar to the upper panel (elevation) whereas the side-scan image will be similar to the bottom panel (plan view).

It is possible to do further analysis of the sub-bottom data to obtain the properties of the sediments more precisely. Inversion techniques can be developed to use the acoustic data for inferring the sediment acoustic properties. Turgut (*17*) and Leblanc et al. (*18*) have developed similar inversion techniques for estimating sediment properties. This involves the development of sophisticated inversion algorithms which is beyond the scope of the present study. The data collected during the present cruises will be analyzed further and inversion schemes will be developed as part of our ongoing research efforts. These inversion schemes will be able to provide sediment information similar to the sediment map shown in Figure 5.

REFERENCES

1. INDOT Division of Research, (2000). *A Field Study of Scour-Monitoring Devices for Indiana Streams*, Technical Summary, FHWA/IN/TRP-2000/13, SPR-2149.
2. Boehmler, E. M., and Olimpio, J. R., (2000). "Evaluation of pier-scour measurement methods and pier-scour prediction with observed scour-measurements at selected bridge sites in New Hampshire, 1995-98," Water Resources Investigations Report 00-4183, USGS.
3. Richardson, E. V, and Davis, S. R, (1995). *Evaluating scour at bridges*, Third Edn., Federal Highway Administration Hydraulic Engineering Circular (HEC) , 18, FHWA-IP-90-017. http://www.fhwa.dot.gov/bridge/hec18SI.pdf
4. Schall, J. D., and Price, G. R., (2004). "Portable scour monitoring equipment," NCHRP Report 515, Transportation Research Board, Washington, D.C.
5. Bath, W. R., (1999). "Remote methods of underwater inspection of bridge structures," FHWA-RD-99-100.
6. Placzek, G., and Haeni, F. P., (1995) "Surface- geophysical techniques used to detect existing and refilled scour holes near bridge piers," USGS Water Resources Investigations Report 95-4009.
7. Trent, R.E., and Friedland, Ian, (1992). "Status of scour instrumentation development", in *Proceedings of the American Society of Civil Engineers Water Forum*, (August 1992) Baltimore, Md.: American Society of Civil Engineers, p. 1088-1093.
8. Lasa, I.R., Hayes, G.H., and Parker, E.T., (2000). "Remote monitoring of bridge scour using echo sounding technology," *Transportation Research Circular*, Issue. 498.
9. US Army Corps of Engineers, (2001). *Engineering Manual: Hydrographic Surveying*, EM 1110-2-1003.
10. Foxworth, M. R. and Reynolds, J, (1995). "Sounding out scour," Civil Engineering, 44-46, December.
11. EdgeTech, (2003). *Integrated side scan sonars and sub-bottom profiler*, Product specifications.

12. Urick, R. J., (1996).*Principles of Underwater Sound*, Peninsula Publications.

13. USGS Woods Hole Center , (undated). *Seafloor mapping: Data Acquisition*, http://woodshole.er.usgs.gov/operations/sfmapping/dataacq.htm

14. Blaha, D., (2000). "Sidescan Sonar as a potential scour inspection tool," Winter Meeting of the Midwest Bridge Maintenance and Inspection Institute, Northwestern University. http://iti.acns.nwu.edu/technology/midwest/november2000/sonar/sld001.htm

15. Kim, H-S and Swanson, J. C. (2001). "Modeling double flood currents in Sakonnet River," Proceedings of the Seventh International Conference on Estuarine and Coastal Modeling, pp. 418-453, ASCE, Reston, Va.

16. Rhode Island Emergency Management Agency, (undated). *Reducing Risks from natural hazards in Narragansett, Rhode Island*, *http://www.riema.ri.gov/nflood.htm*

17. Turgut, A, (1996). "Determination of sub-bottom sediment properties and their spatial distributions from chirp sonar data," *Journal of the Acoustical Society of America*, Volume 99, Issue 4, pp. 2451-2457.

18. Leblanc, L, Mayer, L, Rufino, M, Schock, S. G., and King, J., (1992). "Marine sediment classification using the chirp sonar," *Journal of the Acoustical Society of America*, Volume 91, Issue 1, pp. 107-115.

Appendix: Pier Scour Computation

To determine pier scour, an equation based on the CSU approach is recommended for both live-bed and clear-water pier scour. The equation predicts maximum pier scour depths. The equation is:

$$\frac{y_s}{y_1} = 2.0K_1K_2K_3K_4\left(\frac{a}{y_1}\right)^{0.65} F_{r1}^{0.43} \qquad \text{(A1)}$$

For round nose piers aligned with the flow:

$y_s \leq 2.4$ times the pier width (a) for $Fr \leq 0.8$

$y_s \leq 3.0$ times the pier width (a) for $Fr > 0.8$

In terms of y_s/a, Equation A1 is:

$$\frac{y_s}{a} = 2.0K_1K_2K_3K_4\left(\frac{y_1}{a}\right)^{0.35} F_{r1}^{0.43} \qquad \text{(A2)}$$

where:

y_s = scour depth in m

y_1 =Flow depth directly upstream of the pier, m

K_1 =Correction factor for pier nose shape from Table 1

K_2 =Correction factor for angle of attack of flow from Table 2 or Equation A3

K_3 =Correction factor for bed condition from Table 3

K_4 =Correction factor for armoring by bed material size from Equation A4 and Table 4

a =Pier width in m

L =Length of pier in m

F_{r1} =Froude Number directly upstream of the pier = $V_1/(gy_1)^{1/2}$

V_1 =Mean velocity of flow directly upstream of the pier, m/s

g =Acceleration of gravity (9.81 m/s^2)

The correction factor for angle of attack of the flow K_2 given in Table 3 can be calculated using the following equation:

$$K_2 = \left(Cos\theta + \frac{L}{a}Sin\theta\right)^{0.65} \qquad \text{(A3)}$$

If L/a is larger than 12, use L/a = 12 as a maximum in Equation A3 and Table 3.

TABLE 1. Correction Factor, K_1, for Pier Nose Shape

	Shape of Pier Nose	K_1
1	Square nose	1.1
2	Round nose	1.0
3	Circular cylinder	1.0
4	Group of cylinders	1.0
5	Sharp nose	0.9

TABLE 2. Correction Factor, K_2, for Angle of Attack, θ, of the Flow. Angle = skew angle of flow, L = length of pier, m

Angle	L/a=4	L/a=8	L/a=12
0	1.0	1.0	1.0
15	1.5	2.0	2.5
30	2.0	2.75	3.5
45	2.3	3.3	4.3
90	2.5	3.9	5.0

TABLE 3. Increase in Equilibrium Pier Scour Depths (K_3) for Bed Condition

Bed Condition	Dune Height (m)	K_3
Clear-water scour	N/A	1.1
Plane bed and Antidune flow	N/A	1.1
Small Dunes	$3>H\geq 0.6$	1.1
Medium Dunes	$9>H\geq 3$	1.2 to 1.1
Large Dunes	$H\geq 9$	1.3

The correction factor K_4 decreases scour depths for armoring of the scour hole for bed materials that have a D_{50} equal to or larger than 0.06 m ($D_{50} \geq 0.06$ m). The correction factor results from recent research for FHWA by Molinas at CSU which showed that when the approach velocity (V_1) is less than the critical velocity (V_{c90}) of the D_{90} size of the bed material and there is a gradation in sizes in the bed material, the D_{90} will limit the scour depth. The equation developed by Jones from analysis of the data is:

$$K_4 = \left[1 - 0.89\left(1 - V_R\right)^2\right]^{0.5} \qquad \text{(A4)}$$

where:

$$V_R = \left(\frac{V_1 - V_i}{V_{c90} - V_i}\right)$$

$$V_i = 0.645\left(\frac{D_{50}}{a}\right)^{0.053} V_{c50}$$

$$V_c = 6.19\, y^{1/6} D_c^{1/3}$$

V_R = Velocity ratio
V_1 = Approach velocity, m/s
V_i = Approach velocity when particles at a pier begin to move, m/s
V_{c90} = Critical velocity for D_{90} bed material size, m/s
V_{c50} = Critical velocity for D_{50} bed material size, m/s
a = Pier width, m
D_c = Critical particle size for the critical velocity V_c, m
Limiting K_4 values and bed material size are given in Table 5.

TABLE 4. Limits for Bed Material Size and K_4 Values

Factor	Minimum Bed Material Size	Minimum K_4 Value	V_R>1.0
K_4	**$D_{50}\geq 0.06$ m**	**0.7**	**1.0**

1. The correction factor K_1 for pier nose shape should be determined using Table 1 for angles of attack up to 5 degrees. For greater angles, K_2 dominates and K_1 should be considered as 1.0. If L/a is larger than 12, use the values for L/a = 12 as a maximum in Table 2 and Equation 3.
2. The values of the correction factor K_2 should be applied only when the field conditions are such that the entire length of the pier is subjected to the angle of attack of the flow. Use of this factor directly from the table will result in a significant over-prediction of scour if

(1) a portion of the pier is shielded from the direct impingement of the flow by an abutment or another pier; or

(2) an abutment or another pier redirects the flow in a direction parallel to the pier. For such cases, judgment must be exercised to reduce the value of the K_2 factor by selecting the effective length of the pier actually subjected to the angle of attack of the flow.
3. The correction factor K_3 results from the fact that for plane-bed conditions, which is typical of most bridge sites for the flood frequencies employed in scour design, the maximum scour may be 10 percent greater than computed with Equation 1. In the unusual situation where a dune bed configuration with large dunes exists at a site during flood flow, the maximum pier scour may be 30 percent greater than the predicted equation value. This may occur on very large rivers, such as the Mississippi. For smaller streams that have a dune bed configuration at flood flow, the dunes will be smaller and the maximum scour may be only 10 to 20 percent larger than equilibrium scour. For antidune bed configuration the maximum scour depth may be 10 percent greater than the computed equilibrium pier scour depth.

Width of Scour Holes

The top width of a scour hole in cohesionless bed material from one side of a pier or footing can be estimated from the following equation:

$$W = y_s (K + \cot\theta) \qquad \text{(A5)}$$

where:

W = Top width of the scour hole from each side of the pier or footing, m
y_s = Scour depth, m
K = Bottom width of the scour hole as a fraction of scour depth
θ = Angle of repose of the bed material ranging from about 30° to 44

The angle of repose of cohesiveness material in air ranges from about 30° to 44°. Therefore, if the bottom width of the scour hole is equal to the depth of scour y_s (K = 1), the top width in cohesionless sand would vary from 2.07 to 2.80 y_s. At the other extreme, if K = 0, the topwidth would vary from 1.07 to 1.8 y_s. Thus, the topwidth could range from 1.0 to 2.8 y_s and will depend on the bottom width of the scour hole and composition of the bed material. In general, the deeper the scour hole, the smaller the bottom width. In water, the angle of repose of cohesionless material is less than the values given for air; therefore, a top width of 2.0 y_s is suggested for practical applications.